Journal of Macromolecular Science, Part A
Publication details, including instructions for authors and subscription information:
http://www.informaworld.com/smpp/title~content=t713597274

Synthesis of Iron Oxide Based Gelatin Nanocomposites and their Applications in Removal of Cr (VI) Ions from Aqueous Solutions

Priyanka Agrawal[a]; A. K. Bajpai[a]
[a] Bose Memorial Research Laboratory, Department of Chemistry, Government Autonomous Science College, Jabalpur, M.P., India

Online publication date: 19 November 2010

To cite this Article Agrawal, Priyanka and Bajpai, A. K.(2011) 'Synthesis of Iron Oxide Based Gelatin Nanocomposites and their Applications in Removal of Cr (VI) Ions from Aqueous Solutions', Journal of Macromolecular Science, Part A, 48: 1, 47 — 56
To link to this Article: DOI: 10.1080/10601325.2011.528308
URL: http://dx.doi.org/10.1080/10601325.2011.528308

Journal of Macromolecular Science, Part A: Pure and Applied Chemistry (2011) **48**, 47–56

ISSN: 1060-1325 print / 1520-5738 online
DOI: 10.1080/10601325.2011.528308

Taylor & Francis
Taylor & Francis Group

Synthesis of Iron Oxide Based Gelatin Nanocomposites and their Applications in Removal of Cr (VI) Ions from Aqueous Solutions

PRIYANKA AGRAWAL and A. K. BAJPAI*

Bose Memorial Research Laboratory, Department of Chemistry, Government Autonomous Science College, Jabalpur (M.P.), India

Received May 2010, Accepted July 2010

In the present study, iron oxide based gelatin nanoparticles (FeOGel) have been used as an efficient low cost adsorbent to remove the low concentrations of toxic Cr(VI) ions from aqueous solution. The adsorption experiments were carried out by batch contact method and the effect of the significant process parameters such as initial pH of solution, contact time, adsorbent dose and the initial Cr (VI) concentration were investigated on the metal ion removal capacity. The optimum adsorption of Cr(VI) on the gelatin nanoparticles was observed at an initial pH value of 2-3. The maximum adsorption capacities of FeOGel for Cr(VI) were 120 mg/g at 25°C. The equilibrium sorption data fit satisfactorily to the Langmuir adsorption model. The characterization of the prepared FeOGel was accomplished by FTIR, SEM, TEM, XRD and ζ-potential measurements. The results obtained in this study illustrated that the prepared nanoparticles of iron oxide impregnated gelatin could be an effective and economically viable adsorbents for Cr(VI) removal at low concentration levels from aqueous systems.

Keywords: Adsorption, Cr(VI) removal, iron oxide, gelatin nanoparticles

1 Introduction

Metal ions are nonbiodegradable in nature, and their intake at certain levels are toxic (1). At least 20 metals are classified as toxic and half of these are emitted into the environment in quantities that pose risks to human health (2). One of the major toxic metal ions endangering human life is chromium (VI). Cr (VI) usually occurs as highly soluble and toxic chromate anions ($HCrO_4^-$ or $Cr_2O_7^{2-}$) (3). Cr(VI) has been classified as a Group I human carcinogen by International Agency for Research on Cancer (IARC) and as a Group A inhalation carcinogen by US Environmental Protection Agency (EPA) (4). The maximum chromium levels permitted in wastewater are 5 mg/L for trivalent chromium and 0.05 mg/L for hexavalent chromium. Due to stringent environmental regulations, all the chromium related industries are now facing the issue of disposal of large quantity of wastewater containing toxic metals (5). Industries produce chromium and other heavy metal ions rich aqueous effluents in various processes like electroplating, metal finishing, magnetic tapes, pigments, leather tanning, wood protection, chemical manufacturing, brass, electrical and electronic equipment, catalysis etc. (6). This has deleterious effects on microorganisms, plants, animals and is also carcinogenic to human beings (7). Due to the process of bioaccumulation by aquatic plants and animals, Cr (VI) also persists in marine food chains (8). The removal of this toxic pollutant from the contaminated environments and waste streams is, therefore, of prime importance (9).

A serious problem encountered in the removal of the metal ions is that the target species are usually in low concentration and in complex mixtures (10). The determination of low levels of Cr (VI) in environmental samples and their removal from the water by using an inexpensive processing are very important (11). Several methods have been applied for the removal of toxic metal ions from the industry generated effluents. The common methods currently employed are chemical precipitation, lime coagulation, ion exchange, reverse osmosis and solvent extraction (12). The aforesaid methods have many disadvantages like

*Address correspondence to: A.K. Bajpai, Bose Memorial Research Laboratory, Department of Chemistry, Government Autonomous Science College, Jabalpur (M.P.), 482001, India. Tel: +91 0761 4063754; Fax: (91-761) 262-1272; E-mail: akbmrl@yahoo.co.in; akbajpailab@yahoo.co.in

incomplete metal removal, high reagents and energy requirements and generation of toxic sludge which again needs safe disposal (13).

Adsorption has been extensively studied as a cost-effective technology for the removal of heavy metals from wastewater during the past decades (14). Sorbent plays a key role in the removal of water contaminants since it determines the performance of treatment technology, including adsorption capacity and post-treatment (separation) (15). In recent years, magnetic assisted adsorption separation has emerged as a promising technology employed in water treatment (16). The magnetic sorbents behave similar to or even better than various commercial adsorbents (17). Magnetic adsorbents can be used to adsorb contaminants from aqueous effluents and after adsorption the adsorbents can be separated from the medium by a simple magnetic process (18). In the literature, iron oxides have been found to be successfully used as composite materials with host materials in fabricating magnetic sorbent (19). The main advantages of using iron oxides as composite materials with host materials are the high porosity, magnetic property, and sometimes good settling property (15). Since surface functional group reactions are involved in the sorption processes, higher content of surface functional group sites in a sorbent would greatly lead to higher sorption capacity for removal of contaminants. The host materials to support iron oxides are used to overcome the foregoing problems. The potential host materials are zeolite, alginate, chitosan, clay, and activated carbons (19). Other biopolymeric moieties capable of interacting with the metal ions are proteins, which because of nitrogen atoms of the imidazole group of the histidine residue and the sulfhydryl group of the fine cysteine residue are potential adsorbent for metal ions (10).

Thus, the objective of this study was to synthesis and characterization of environment friendly iron oxide based gelatin nanoparticles for the removal of Cr (VI) from aqueous solutions. For this purpose, the prepared iron oxide impregnated gelatin nanoparticles were characterized by spectroscopic and microscopic characterization methods like FTIR, SEM TEM and XRD and used to investigate the removal of chromium from aqueous solutions.

2 Experimental

2.1 Materials

Gelatin (acid processed) was purchased from Loba Chemie, India and used without further treatment. Other chemicals such as potassium dichromate (adsorbate), glutaraldehyde (crosslinking agent for gelatin), ferrous and ferric chloride, sodium hydroxide and hydrochloric acid, acetone and toluene were used of high purity grade. Doubly distilled water was used throughout the experiments.

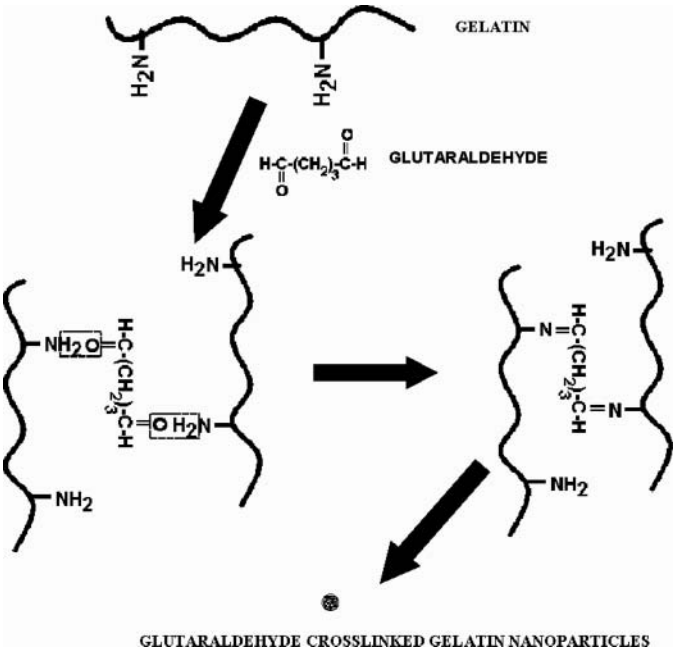

Fig. 1. Schematic representation of crosslinking reaction between gelatin and glutaraldehyde.

2.2 Methods

2.2.1. *Preparation of Adsorbent Gelatin Nanoparticles*

The gelatin based nanoparticles were prepared following an emulsion crosslinking method. In the first step, the known volumes of aqueous solutions of gelatin and glutaraldehyde (crosslinker) were shaken separately in the presence of an oil phase to form a stable emulsion. The crosslinker (glutaraldehyde) emulsion was then added dropwise to gelatin emulsion while stirring so that the crosslinked nanoparticles of gelatin were prepared. The reaction was allowed to take place for a definite time period to observe complete crosslinking. The particles so prepared were precipitated, washed and dried. The crosslinking reaction of gelatin with glutaraldehyde is shown in Figure 1.

2.2.2. *Preparation of Iron Oxide Gelatin Nanocomposites*

The gelatin nanoparticles prepared as above were allowed to swell in a solution of Fe^{2+}/Fe^{3+} ions of known concentration. After equilibrium swelling is achieved the Fe^{2+}/Fe^{3+} impregnated gelatin nanoparticles are left in an alkali (NH_4OH) bath so that the Fe^{2+}/Fe^{3} ions get precipitated into iron oxide within the nanoparticles matrix. The prepared iron oxide gelatin nanocomposites were thoroughly washed dried and stored in airtight containers. The *in situ* precipitation of iron oxide within the matrix of gelatin nanoparticles may be presented as below (20):

$$2FeCl_3 + FeCl_2 + 8NH_4OH \rightarrow Fe_3O_4 + 8NH_4Cl. \quad (1)$$

2.2.3. *Preparation of Synthetic Adsorbate Samples*

A stock solution of Cr(VI) (1000 mg/L) was prepared by dissolving an appropriate quantity of AR grade $K_2Cr_2O_7$ (Merck India Ltd.) in 1000 mL of distilled water. The stock solution was further diluted with deionized water to a desired concentration for obtaining the test solutions.

2.2.4. *Protocol of Adsorption Experiments*

The adsorption experiments were carried out in batch mode at ambient temperature. In order to investigate the nature of Cr (VI)-FeOGel interaction, initially the effect of pH on percentage removal was carried out and then further experiments on the effect of agitation time, initial concentration and adsorption dosage were conducted by using optimized pH. Only one parameter was changed at a time while others were maintained as constant. In the first set of experiments, percentage adsorption was studied at various pH ranging from 1–8 at FeOGel of 0.2 g/20 mL, initial Cr(VI) concentration of 1.0 mg/L and the predetermined time (90 min) in a rotary shaker at a speed of 160 rpm using a series of clean 250 mL conical flasks. Next, a second set of experiments were conducted with various agitation times, various initial Cr(VI) concentration (from 0.5 to 2.0 mg/L) at constant adsorbent (0.2 g/20 mL) dose and at optimized pH 2.0. In the third set of experiments, the FeO gel dose was varied (0.2–1.0 g/20 mL) while other parameters such as initial Cr(VI) concentration (1 mg/L), optimum time (90 min) and optimum solution pH remained constant. After completion of every set of experiments, the supernatants were stored for residual chromium analysis. The pH of each solution was adjusted using the required quantity of 0.1N HCl (or) 0.1N NaOH before mixing the adsorbent.

2.2.5. *Cr (VI) Estimation by Diphenylcarbazide Method*

The amount of adsorbed Cr(VI) was measured spectrophotometrically by the diphenylcarbazide method and the Cr(VI) content in supernatant was estimated after adding 6N H_2SO_4, a solution of 1,5-diphenylcarbazide in acetone and measuring the absorbance at 540 nm using a systronic-106 spectrophotometer. The method displayed a linear relation with 10–100 μg of Cr(VI) and the calibration graphs used displayed r^2 values of 0.9998. The metal uptake (qe) was calculated by mass balance expression:

$$\text{qe} = (\text{Co} - \text{Ce})\text{v}/\text{m} \tag{2}$$

where qe (mg/g) is the amount of chromium adsorbed, Co is the initial metal concentration (mg/L), C_f and Ce are the final residual concentrations of chromium (mg/L) after adsorption at time 't' and at equilibrium time, respectively, v is the volume of aqueous solution (mL) and m is the weight of swollen adsorbent (g). The % removal of chromium from aqueous solution was estimated using the following equation:

$$\%\,\text{Removal} = \text{Co} - \text{Cf} \times 100/\text{Co} \tag{3}$$

2.2.6. *Fourier Transform Infrared (FTIR) Spectroscopy*

The FTIR spectra of unadsorbed crosslinked iron oxide impregnated gelatin nanoparticles and Cr (VI) adsorbed nanocomposite of gelatin were recorded on a FTIR-8400S, Shimadzu spectrophotometer. Prior to analysis, KBr pellets were prepared by mixing 1:10 of sample: KBr (wt/wt) followed by uniaxial pressing the powders under vacuum. Spectra were obtained between 4000–400 cm^{-1} at 2 cm^{-1} resolution.

2.2.7. *SEM Analysis*

To examine the morphological characteristics of the nanoparticles, samples were viewed using a scanning electron microscope (STEREO SCAN, 430, Lecica SEM, USA).

2.2.8. *TEM Analysis*

The particles size determination was carried out using the TEM images. Transmission electron microscopy (TEM) was performed by using a Morgagni-268-D transmission electron microscope with an acceleration voltage of 80.0 kv. The samples prepared for the TEM measurement were done by dispersing a drop of the sample solution on Formvar-coated C grids.

2.2.9. *XRD Analysis*

The crystalline nature of the bare gelatin nanoparticles and iron oxide incorporated gelatin nanoparticles was studied on a rotating X-ray diffractometer (IUC DAE, Indore) scans at 0.005 deg (2θ)/s in the 2θ range 10–60°.

2.3 Zeta Potential Measurements

The surface charge measurement is an important adsorption influencing parameter. As the FeOGel nanoparticles were prepared by the physicochemical process, the electrostatic nature of these nanoparticles changes with different pH of immersion medium. The surface charges were measured by suspending 0.2 g of the swollen FeO gelatin nanoparticles into the aqueous medium of varying pH and measuring the surface charge by a pH/E.M.F. meter (Systronics μpH system-362).

3 Results and Discussion

3.1 IR Spectra Analysis

The IR spectra of iron oxide incorporated gelatin particles (Fig. 2(a)) before and after chromium adsorption (Fig. 2(b)), were recorded to acquire the information regarding wave number changes (peak shifting) of the functional groups in the range of 400–4000 cm^{-1}. Table 1 presents some of the basic band frequencies of gelatin and Cr(VI) as dichromate. A very broad peak at 3100 cm^{-1}–3600 cm^{-1} corresponds to vibrational bands of O–H probably

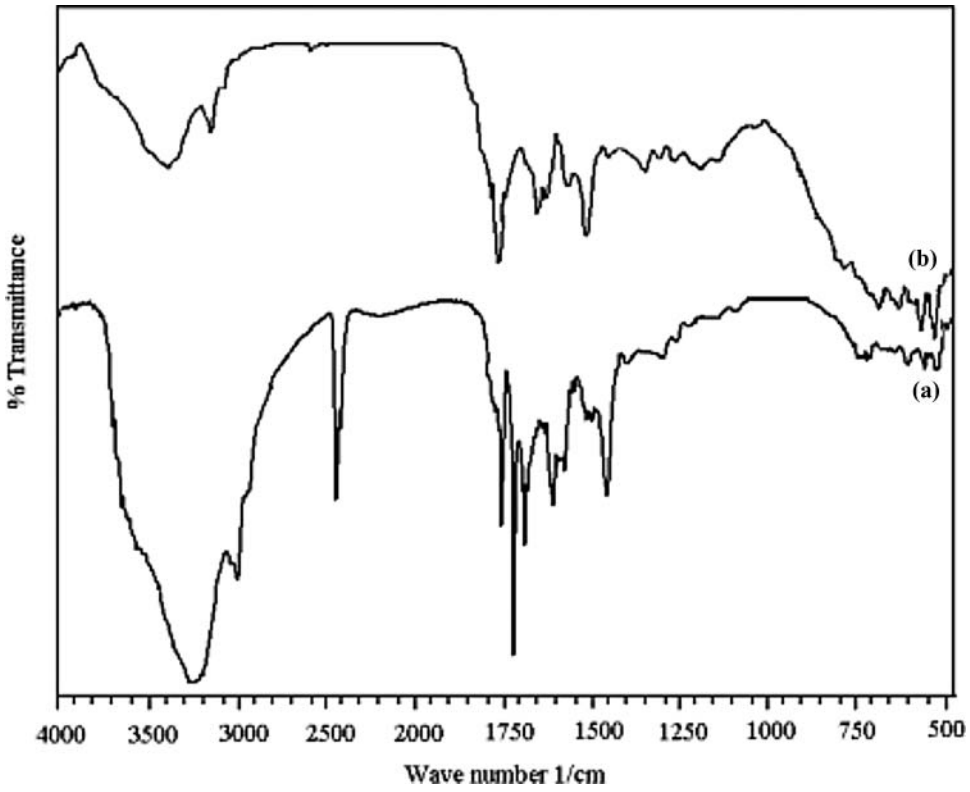

Fig. 2. FTIR spectra of (a) FeO-gelatin nanoparticles, and (b) Cr(VI) adsorbed FeO-gelatin nanoparticles.

indicating the presence of surface hydroxyl groups (Fe-OH_2) and the carboxyl groups of gelatin (21). The presence of amino groups of gelatin in the spectra is indicated by NH_3 stretching band at 2365 cm^{-1} and amide I mode of peptide bond at 1633 cm^{-1}. The IR spectra also mark the presence of methylene groups due to asymmetric stretch of CH_2 groups. More importantly, the presence of two new peaks corresponding to iron oxide appeared at 578 and 427 cm^{-1} (22) and O–Cr–O bridging frequency of $Cr_2O_7^{2-}$ ion appears at 770–790 cm^{-1} (23).

3.2 SEM Characterization

The surface morphology of the gelatin nanoparticles was visualized by a scanning electronic microscope. The purpose of the SEM study was to examine the surface microstructure of the sorbents. Figure 3 reveals the smooth, homogeneous, relatively spherical particle surfaces for the toxic metal adsorption.

3.3 TEM Characterization

The TEM images show the relatively spherical structure and the narrow size distribution of the FeOGel (Fig. 4(a)) and the Cr(VI) adsorbed FeOGel nanocomposites (Fig. 4(b)), demonstrates the dark core of the Cr(VI) around the FeOGel nanoparticles. According to these images the average size of bare FeOGel nanoparticles is 28.48 nm, while that of metal adsorbed particles is between 38.19 to 45.24 nm.

Table 1. FTIR data of iron oxide impregnated gelatin nanoparticles and Cr(VI) adsorbed FeO-gelatin nanoparticles composite

Type	*Frequency cm^{-1}*	*Assignment*
1. FeO-gelatin nanoparticles	3200 cm^{-1}–3600 cm^{-1}	O–H, N–H strch band (21) amide-I, C=O strach
	1642 cm^{-1}	
	1533 cm^{-1}	N–H deformation amide-II
	578 cm^{-1}	
		Fe–O vib. Bands (22)
	427 cm^{-1}	
2. Cr(VI) adsorbed FeO-gelatin nanoparticles	770–790 cm^{-1}	O–Cr–O bridging frequency of $Cr_2\ O_7^{2-}$ (23)

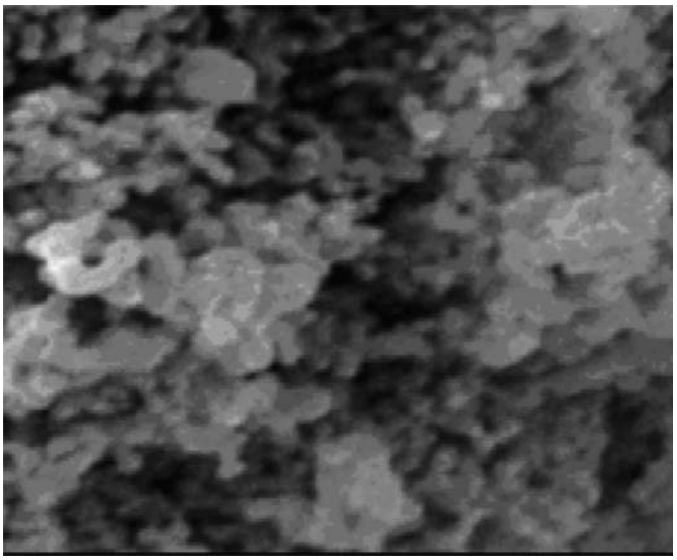

Fig. 3. SEM image of FeO-gelatin nanoparticles.

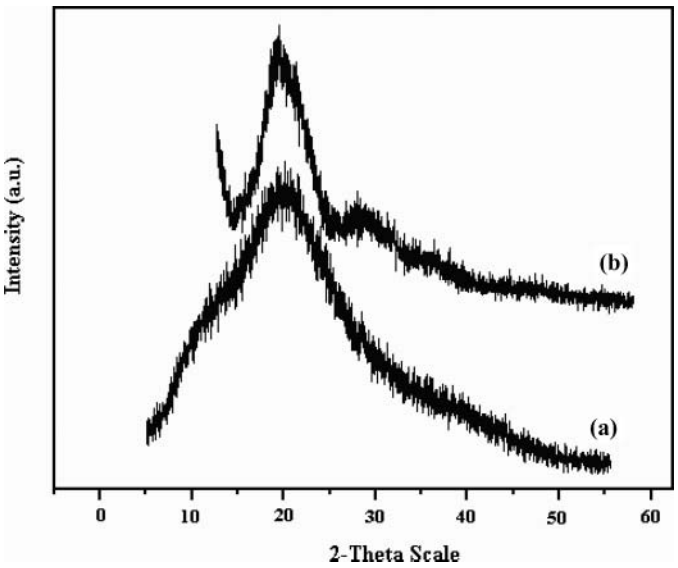

Fig. 5. XRD pattern of glutaraldehyde crosslinked nanoparticles of (a) gelatin, and (b) iron oxide loaded gelatin nanoparticles composite.

3.4 XRD Analysis

The XRD patterns of the prepared gelatin nanoparticles and iron oxide imprgegnated gelatin nanocomposite are shown in Figure 5(a) and (b), respectively. In the XRD spectra of gelatin nanoparticles the appearance of broad peak indicates the amorphous nature of gelatin (Fig. 5(a)) and in (Fig. 5(b)) the appearance of a new small peak at 30.24 suggests the impregnation of iron oxide into gelatin nanoparticles which is in agreement with γ-Fe_2O_3 standard data (24). The amorphous and crystalline nature of the gelatin nanoparticles and iron oxide impregnated gelatin nanocomposites are also determined by the degree of crystallinity. The numerical formula to calculate the percent crystallinity of gelatin nanoparticles and FeOGel nanocomposites is given in the following equation:

$$\mathrm{Xc}\,(\%) = (\mathrm{Ac}/\mathrm{Aa} + \mathrm{Ac}) \times 100 \qquad (4)$$

where Ac and Aa are the area of crystalline and amorphous phases, respectively (25). The percent crystallinity of the bare gelatin nanoparticles and FeOGel nanocomposites were calculated to be approximately 8.59% and 39.08%, respectively. Since gelatin is amorphous in nature and an overall increase in percent crystallinity clearly suggests the impregnation of iron oxide in the gelatin nanoparticles.

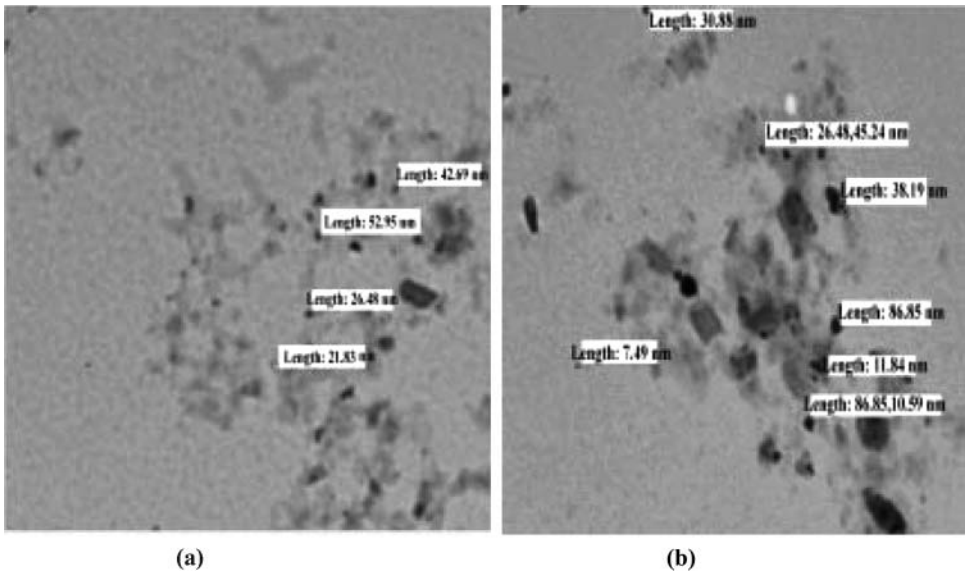

Fig. 4. TEM images of bare (a) FeO-gelatin nanoparticles, and (b) TEM images of FeO-gelatin nanoparticles after Cr(VI)l adsorption.

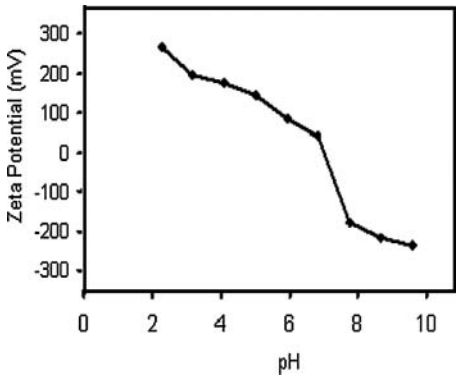

Fig. 6. Variation of the surface charge onto nanoadsorbent at different pH, Temp = 25°C, nanoparticles = 0.2 g, Time = 90 min, Cr(VI) solution 20 mL of initial conc.1 mg/L.

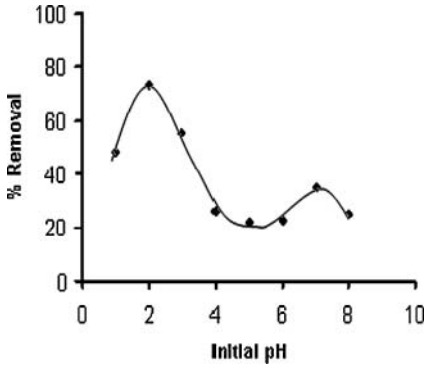

Fig. 7. The effect of initial pH on % removal of Cr(VI) Temp = 25°C. pH = 2.0, nanoparticles = 0.2 g, Time = 90 min, Cr(VI) solution 20 mL of initial conc. 1 mg/L.

The mean grain size was calculated using Debye-Scherrer formula (26) is given in the following equation:

$$d = k\lambda/\beta\cos\theta \quad (5)$$

where d is mean grain size, k is the shape factor (0.9), β is broadening of the diffraction angle and λ is diffraction wavelength (1.54 Å). The estimated average grain size of FeO-gelatin nanoparticles was found to be 8 nm, which is in agreement with the TEM analysis results.

3.5 Zeta Potential Measurements

The stability of FeOGel nanoparticles in aqueous medium depends on its surface charge, therefore ζ-potential measurements can be employed as an indicator of their surface charge. Figure 6 shows the ζ-potential values of FeOGel nanoparticles as a function of pH. The titration curve obtained by adding HCl to an aqueous suspension of FeOGel nanoparticles shows a decrease of the ζ-potential from 220 to-280 mV, while changing the pH from 10 to 1. This change in the surface potential can be attributed to the surface hydroxyl group $FeOH_2^+$ of the iron oxide impregnated gelatin nanoparticles (27). In the basic environment, the surface shows a negative potential due to the formation of FeO^-, while in the acidic environment, a positive surface charge is expected due to $FeOH_2^+$ formation. Unlike these results, which demonstrate a point of zero charge (PZC) at pH 6.8 (28) reported a PZC of γ-Fe_2O_3 nanoparticles at pH 7.3. The PZC at lower pH can be attributed to the iron oxide –gelatin interaction. In this way, the surface charge at acidic medium due to $FeOH_2^+$ suggests the maximum Cr(VI) adsorption.

3.6 Effect of Initial pH

To investigate the effects of pH on adsorption, the initial pH values were adjusted to the range of 2.0–9.0 before the addition of the adsorbent into the solution. The initial Cr (VI) concentration was set at 1 mg/L and the agitation time was 90 min. Figure 7 shows the effect of pH on percentage adsorption of chromium. It can be seen from Figure 7 that the adsorption of Cr (VI) decreased with an increase in the initial pH from 2.0 to 8.0. The maximum removal occurred at the initial pH 2-3 for FeOGel nanoparticles. A dramatic decrease was noticed at pH 4-5, followed by a gradual decrease and sudden increase in the pH range of 4–9, which may be due to the fact that at lower pH the surface area of the adsorbent was more protonated due to cationic monomeric form ($FeOH_2^+$) and competitive negative ions adsorption occurred between positive surface and free chromate ions. Adsorption of Cr(VI) at pH 2.0 shows that the binding of the negatively charged chromium species ($HCrO_4^-$) occurred through electrostatic attraction to the positively charged surface hydroxyl groups $FeOH_2^+$ of the iron oxide coated gelatin nanoparticles. However, in highly acidic medium (pH ≈1) H_2CrO_4 (neutral form) is the predominant species of Cr (VI) as reported elsewhere (29). Hence, at pH 1.0 percentage adsorption decreased due to the involvement of less number of $HCrO_4^-$ anions on the positive surface. At higher pH, due to a greater number of FeO^- ions, adsorbent surface carries net negative charges, which tend to repel the metal anions (CrO_4^{2-}) (30). However, there is also some percentage removal at pH >2.0, but the rate of adsorption is reduced. This might be due to the weakening of electrostatic forces of attraction between the oppositely charged adsorbate and adsorbent or physisorption due to weak undirected Van der Waals forces of attraction (31, 32). Considering the removal efficiency of FeOGel nanoparticles remained at a low level throughout the whole pH range, all subsequent adsorption experiments herein were conducted at pH 2, the optimum pH for adsorption of Cr(VI) ions on FeOGel nanoparticles.

3.7 The Effect of Agitation Time and Initial Metal Ion Concentration

Equilibrium time is an important parameter for an economical wastewater treatment process. Figure 8 depicts the

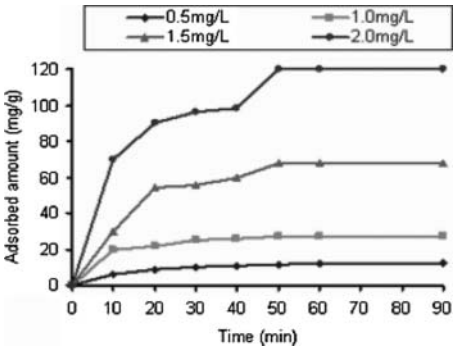

Fig. 8. The effect of agitation time on initial concentration range (0.5–2.0 mg/L), Temp. = 25°C, pH = 2.0, nanoparticles = 0.2 g, Time = 90 min, Cr(VI) solution 20 mL.

effect of agitation time on the removal efficiency of Cr (VI) at various initial concentrations (0.5-2.0 mg/L) by FeOGel nanocomposites. A two stage behavior is observed. It is observed from the results that the uptake of Cr(VI) ions is initially quite high, and slows down with the lapse of time leading gradually to an equilibrium condition. It also shows that a major fraction of Cr(VI) ions is adsorbed onto FeOGel nanoparticles during the first 50 min, while only a very small part of the additional adsorption occurs during the following contact time, indicating that during the initial stage of the process there are plenty of readily accessible sites available for increasing the rate of adsorption. As time lapses, the surface coverage increases, the rate of uptake become slower in latter stages, and ultimately an almost plateau region is attained when surface become saturated. It has to be noted from Figure 8 that the equilibrium is attained around 60 min. In order to get the maximum uptake, the agitation was determined 90 min. during the batch studies. Similar types of observations have been reported elsewhere (33).

The effect of initial concentration on percentage removal can also be seen in Figure 9. The percentage removal decreased from 88% to 65% as the initial concentration of Cr(VI) is increased from 0.5 to 2.0 mg/L for 0.2 g/20 mL

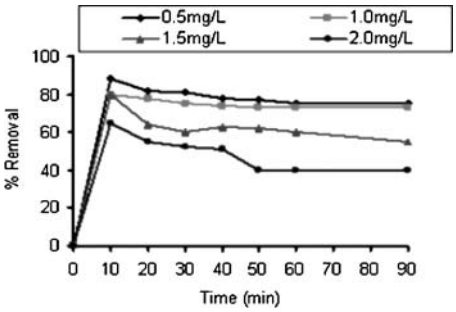

Fig. 9. The effect of initial concentration (0.5, 1.0, 1.5, 2.0 mg/L) on % removal of Cr(VI), Temp = 25°C, pH = 2.0, nanoparticles = 0.2 g, Time = 90 min, Cr(VI) solution 20 mL.

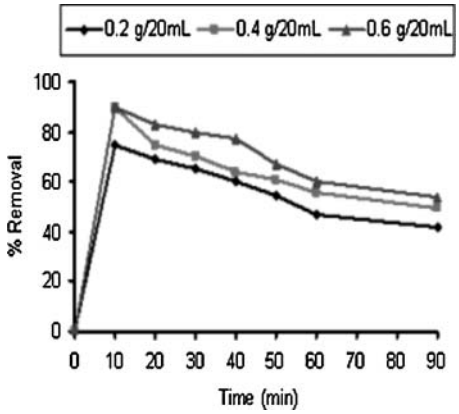

Fig. 10. The effect of adsorbent dose on the adsorption of Cr(VI), Temp. = 25°C, pH = 2.0, nanoparticles = 0.2 g, 0.4 g, 0.6 g, Time = 90 min, Cr(VI) solution (Conc. 1 mg/L) 20 mL.

of adsorbent at equilibrium contact time of 90 min. Interestingly, it has been seen that the adsorption capacity of the unit mass of the adsorbent (0.2 g) found to increase from 12 to120 mg/g as the Cr(VI) concentration increased from 0.5 to 2.0 mg/L. Similar types of observations have been reported by (34) for Cr(VI) removal using jatropha oil cake, sugarcane bagasse and maize corn cob. This may be due to the fact that the increased Cr(VI) concentrations provide the maximum driving force to overcome all the mass transfer resistances of metal ions from the aqueous phase to solid phase resulting in higher probability of collision between metal ions and the active sites (32).

3.8 The Effect of Adsorbent Dosage

The influence of adsorbent dosage on Cr (VI) sorption was studied by varying the amount of adsorbent from 0.2 to 0.6 g. Figure 10 depicts that the percentage removal of chromium increased from 75% to 90% with an increase of adsorbent dosage from 0.2 to 0.6 g/20 mL solution. This trend is obvious because as the adsorbent dose increases the number of adsorbent particle also increases, that makes the greater availability of exchangeable sites for adsorption. Similar types of observations have been reported on Cr(VI) sorption (10).

3.9 The Effect of Solid to Liquid Ratio

The solid to liquid ratio in an adsorption system exerts a great effect on the amount of adsorbed solute particles. A change in solid to liquid ratio not only changes the number of active sites available on the adsorbate but also brings about a change in the number of ions of the solute invading the solid surface for adsorption. In the present study, the solid to liquid ratio has been varied in the range of 0.1–1.0 (g/mL) and the respective results are shown in Figure 11, which clearly reveal that the amount of adsorbed

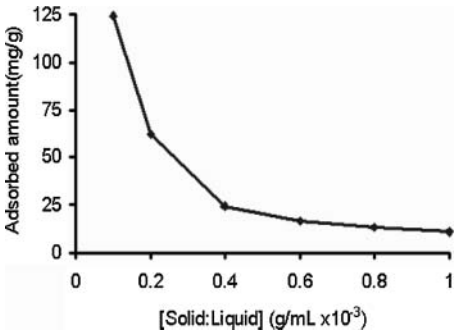

Fig. 11. The effect of solid: liquid (varying amount of solid) on adsorbed amount (mg/g) on adsorption of Cr(VI), Temp. = 25°C, pH = 2.0, nanoparticles = 0.2 g, Time = 90 min, Cr(VI) solution 20 mL of initial conc. 1 mg/L.

Cr(VI) ions decreases with increasing solid to liquid ratio. The results may be explained on the basis of the fact that due to the increasing amount of FeOGel nanoparticles in the adsorption system, their larger surfaces remain inaccessible to the adsorbing Cr(VI) ions, thus lowering the amount of adsorbed Cr(VI) ions. Similar type of observations has been published elsewhere (10).

3.10 Sorption Equilibrium Study

In order to optimize the design of an adsorption system for removal of Cr(VI) from solutions, it is essential to establish the most appropriate correlation for the equilibrium curve. The most common type of isotherms is the Langmuir model. The Langmuir isotherm is based on the assumption that there is a finite number of binding sites, which are homogeneously distributed over the adsorbent surface. These binding sites have the same affinity for adsorption of a single molecular layer so that there is no interaction between adsorbed molecules. The Langmuir isotherm given in Equation 6 gave the best fit of the experimental data:

$$qe/Ce = (QobCe/1 + bCe) \quad (6)$$

$$qe = 1/Qob + Ce/Qo \text{ (linear form)} \quad (7)$$

where qe is the amount of chromium ions adsorbed per unit mass of adsorbent (mg/g), Ce is the equilibrium concentration of metal ions (mg/L), Qo is a measure of adsorption capacity of adsorbent (mg/g), *b* is the Langmuir constant which is a measure of energy of adsorption (L/mg). The experimental data were fitted into Equation 7 for linearization by plotting Ce/qe against Ce and a good fit of this equation reflects monolayer adsorption. The values of Qo and *b* obtained in this work presented in (Table 2) were 28 $\times$ 10^{-3}mg/g and 4.55 L/mg, respectively. The separation factor or equilibrium constant (R_L) is represented by:

$$R_L = (1/1 + bCo) \quad (8)$$

where Co is the initial concentration of Cr(VI) ions (mg/L) and *b* is the Langmuir constant which indicates the nature of adsorption. The separation factor (R_L) indicates the isotherm shape and whether the adsorption is favorable or not. If $R_L = 0$, adsorption is irreversible; $0 < R_L < 1$, adsorption is favorable; $R_L = 1$ adsorption is linear and $R_L > 1$ adsorption is unfavorable. The R_L factor for various initial concentrations of Cr(VI) sorption on FeOGel obtained in this work was in the range of $0 < R_L < 1$ and is presented in Table 3. These values are in very good agreement with the reported values in the literature (23, 35). Alternatively, the Freundlich empirical equation was chosen to describe the exponential distribution of active centers, characteristic of heterogeneous surface and infinite surface coverage. The Freundlich equation is commonly represented by:

Table 2. Data showing the adsorption isotherm values

	Langmuir constants			*Freundlich constants*		
Adsorbent	Q_0 *(mg/g)*	*b (L/mg)*	R^2	*K (mg/g)*	*1/n*	R^2
FeO-gelatin	28×10^{-3}	4.55	0.9993	−2.799	0.5508	0.8653

$$qe = KCe^{1/n} \quad (9)$$

$$\log qe = \log K + 1/n \log Ce \text{ (linear form)} \quad (10)$$

where K is the measure of adsorption capacity and $1/n$ adsorption intensity. From Table 2, the value of the correlation coefficient (R_2) for the Langmuir equation (0.9993) is much higher than that for the Freundlich equation (0.8653). Thus, the adsorption data fit well to the Langmuir isotherm. Slope and intercept give the values of $1/n$ and K. Freundlich constants are also presented in Table 2. The value of $1/n$ is less than 1 and indicates a favorability of adsorption. The Freundlich equation frequently gives an adequate description of adsorption data over a restricted range of concentration, even though it is not based on the theoretical background. These values are in fairly good agreement with the reported values in the literature (24).

3.11 Adsorption Mechanism

On the basis of the adsorption studies in performed aqueous solution, the distribution of the Cr(VI) species mainly depends on solution pH and Cr(VI) concentration

Table 3. Data showing the R_L values

Initial concentration (mg/L)	R_L *value*
0.5	0.305
1.0	0.18
1.5	0.127
2.0	0.099

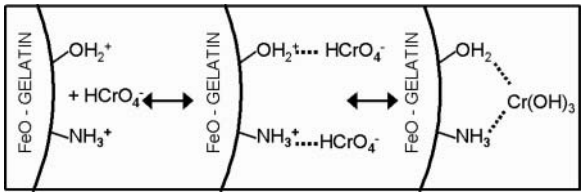

Fig. 12. The potential sorption mechanism of Cr(VI) onto FeO-gelatin nanoparticles composite.

according to the following equilibrium equation:

$$\begin{array}{ccccc} & & \log K = 0.382 & \log K = -6.14 & \\ \mathbf{H_2CrO_4} & \leftrightarrow & \mathbf{HCrO_4^-} & \leftrightarrow & \mathbf{CrO_4^{2-}} \\ & & \uparrow\downarrow \log K = 1.706 & & \\ & & \mathbf{Cr_2O_7^{2-}} & & \end{array} \quad (11)$$

At pH values under 3.0, the acid chromate ion species ($HCrO_4^-$) were predominant in solution (36). The possible mechanism (Fig.12) of the adsorption process of FeOGel towards Cr (VI) consists of two steps: (1) the binding of $HCrO_4^-$ to the positively charged $FeOH_2^+$ groups present on the adsorbent surface and (2) the chemical bonding between $HCrO_4^-$ and adjacent functional groups of the adsorbent.

4 Conclusions

In this study, a novel nanocomposite adsorbent comprising gelatin nanoparticles impregnated with iron oxide was successfully prepared for removing Cr (VI) from aqueous solution. The FTIR characterization clearly shows the impregnation of iron oxide and adsorption of Cr(VI) ions in the prepared FeOGel nanocomposites. In the XRD studies, % crysatallinity results clearly indicate the amorphous nature of gelatin nanoparticles and crystalline nature of iron oxide FeOGel nanoparticles, and the mean grain size 8nm of the FeOGel nanocomposites was in fair agreement with the TEM analysis results. The SEM and TEM studies reveal the smooth, homogeneous, relatively spherical structure and the narrow size distribution of the iron oxide in gelatin nanoparticles. The surface potential measurements and pH studies indicate that the optimum Cr(VI) sorption can be achieved at initial solution pH 2-3. The batch adsoption tests determined the effectiveness of sorptive material as it reaches equilibrium within 60 min and 70% of Cr(VI) ions being adsorbed at 20 min. Adsorption equilibrium studies show that Cr(VI) adsorption data follow the Langmuir model. The maximum adsorption capacity of FeOGel was determined to be 120 mg/g and is considered higher than that of other reported magnetic adsorbents (37). Consequently, the experimental results suggest that, as a kind of potential adsorbent, the FeOGel can remove heavy metals from wastewater efficiently using the technology of magnetic separation and that this process can be competitive with the conventional technologies.

Acknowledgements

The authors wish to thank the UGC –DAE, Consortium for Scientific Research, (Indore, India) for their aid in the XRD and to the authorities of AIIMS (All India Institute of Medical Sciences), Delhi (India) for carrying out SEM and TEM analysis. The authors also wish to thank Dr. O. P. Sharma, HOD, Department of Chemistry, Govt. Science College, Jabalpur, for providing FTIR facilities available in the Chemistry Department.

References

1. Bose, P., Bose, A. and Kumar, M.S. (2002) *Adv. Environ. Res.*, 7, 79–195.
2. Oliveira, L.C.A., Rios, R.V.R.A., Fabris, J.D., Sapag, K., Garg, V.K. and Lago, R.M. (2003) *Appl. Clay Sci.*, 22, 169–177.
3. Park, D., Yun, Y.S., Lim, S.R. and Park, J.M. (2006) *J. Microbiol. Biotechnol.*, 16, 1720–1727.
4. Hamadi, N.K., Chen, X.D., Farid, M.M. and Lu, M.G.Q. (2001) *Chem. Eng. J.*, 84, 95–105.
5. Lakshmanraj, L., Gurusamy, A., Gobinath, M.B. and Chandramohan R. (2009) *J. Hazard. Mater.*, 169, 1141–1145.
6. Mohan, D. and Pittman, Jr., C.U. (2006) *J. Hazard. Mater. B.*, 137, 762–811.
7. Hosseini, M. S., Hosseini-Bandegharaei, A., Raissi, H. and Belador, F. (2009) *J. Hazard. Mater.*, 169, 52–57.
8. Banerjee, S.S. and Chen, D.H. (2007) *J. Hazard. Mater.*, 147, 792–799.
9. Chun, C.L., Hozalski, R.M. and Arnold, T.A. (2005) *Environ. Sci. Technol.*, 39, 8525–8532.
10. Bajpai, J., Shrivastava, R. and Bajpai, A.K. (2007) *J. Appl. Polym. Sci.*, 103, 2581–2590.
11. Chen, W., Zhong, G., Zhou, Z., Wu, P. and Hou, X. (2005) *Anal. Sci.,* 21, 1189–1193.
12. Ozturk, N. and Kavak, D. (2005) *J. Hazard. Mater.*, 127, 81–88.
13. Yazicigil, Z. and Oztekin,Y. (2006) *Desalination*, 190, 71–78
14. Davis, T.A., Volesky, B. and Mucci, A. (2003) *Water Res.,* 37, 4311–4330.
15. Lim, S.F., Zheng, Y.M., Zou, S.W. and Chen, J.P. (2009) *Chem. Eng. J.,* 152, 509–513.
16. Peng, X., Luan, Z. and Zhang, H. (2006) *Chemosphere*, 63, 300–306.
17. Nah, I.W., Hwang, K.Y., Jeon, C., Choi, H.B. (2006) *Miner. Eng.*, 19, 1452–1455.
18. Liu, H., Qing, B., Ye, X., Li,Q., Lee, K., Wu, Z. (2009) *Chem. Eng. J.,* 151, 235–240.
19. Chang, Y.C., Chang, S.W. and Chen, D.H. (2006) *Funct. Polym.*, 66, 335 – 341.
20. Zargar, B., Parham, H. and Hatamie A. (2009) *Chemosphere,* 76, 554–557.
21. Bouguslavsky, Y. and Margel, S. (2008) *J. Colloid Interface Sci.*, 317, 101–114.
22. Gaihre, B., Aryal, S., Barakat, N.A.M. and Kim, H.Y. (2008) *Mater. Sci. Eng. C.*, 28, 1297–1303.
23. Bajpai, J., Shrivastava, R. and Bajpai, A.K. (2004) *Colloids Surf. A: Physicochem. Eng. Aspects.*, 236, 81–90.
24. Zhou, Y.T., Nie, H.L., White, C.B., He, Z.Y. and Zhu, L.M. (2009) *J. Colloid Interf. Sci.*, 330, 29–37.

25. Gupta, R. and Bajpai, A.K. (2010) *J. Biomat. Sci.*, 1–26 (*in press*).
26. Bundela, H. and Bajpai, A.K. (2008) *Exp. Polym. Lett.*, 2, 201–213.
27. Hunter, R.J. Foundations of Colloid Science, Oxford Univ. Press: New York, p. 361, 2000.
28. Ponton, A., Bee A., Talbot, D. and Perzynski, R. (2005) *J. Phys. Condens. Matter*., 17, 821–836.
29. Agrawal, A., Pal, C. and Sahu, K.K. (2008) *J. Hazard. Mater.*, 159, 458–464.
30. Amarasinghe, B.M.W.P.K. and Williams, R.A. (2007) *Chem. Eng. J.*, 132, 299–309.
31. Mohanty, K., Jha, M., Meikap, B.C. and Biswas, M.N. (2005) *Chem. Eng. Sci.,* 60, 3049–3059.
32. Baral, S.S., Das, S. N. and Rath, P. (2006) *Biochem. Eng. J.*, 31, 216–22.
33. Ren, Y.M., Wei, X.Z. and Zhang, M.L. (2008) *J. Hazard. Mater.,* 158, 14–22.
34. Garg, U.K., Kaur, M.P., Garg, V.K. and Sud, D. (2007) *J. Hazard. Mater.,* 140, 60–68.
35. Meena, A.K., Kadirvelu, K., Mishra, G.K., Chitra, R. and Nagar, P.N. (2008) *J. Hazard. Mater.,* 150, 604–611.
36. Cimino, G., Passerini, A. and Toscano, G. (2000) *Water Res.,* 34, 2955–2962.
37. Zhou, L.M., Wang, Y.P., Liu Z.R. and Huang, Q.W. (2006) *Acta Phys. Chim. Sin.,* 22, 1342–1346.